Electronic Supplementary Material (ESI) for Dalton Transactions.
This journal is © The Royal Society of Chemistry 2021

Supporting Information

pH-dependent formation of three porous In(III)-MOFs: framework diversity and selective gas adsorption

Chengcheng Zhang,[a‡] Yuanyuan Qin,[a‡] Lijuan Duan,[a] Lu Wang,[a] Yuewei Wu,[a] Yan Guo,[a*] Weiming Song[a] and Xiangyu Liu[a,b*]

[a] State Key Laboratory of High-efficiency Utilization of Coal and Green Chemical Engineering, National Demonstration Center for Experimental Chemistry Education, College of Chemistry and Chemical Engineering, Ningxia University, Yinchuan 750021, China.

[b] State Key Laboratory of Coordination Chemistry, Nanjing University, Nanjing, 210023, China.

‡ These authors contributed equally to this work.

***Corresponding author**

Dr. Xiangyu Liu

E-mail: xiangyuliu432@126.com

***Corresponding author**

Dr. Yan Guo

E-mail: 452785231@qq.com

Contents:

1. Experimental section

Materials and Methods.

All reagents used for the synthesis were purchased from commercial sources and used without further purification. Elemental analyses of C, H and N were performed on a Vario EL III analyzer. Infrared (IR) spectra were recorded on a Bruker FTTR instrument with KBr pellets (4000-400cm^{-1}). The thermogravimetric analysis (TGA) on **NXU-1** (6.86 mg), **NXU-2** (5.48 mg) and **NXU-3** (4.80 mg) were performed using a CDR-4P thermal analysis system under a N_2 atmosphere from room temperature to 900 °C at a ramping rate of 10 °C/min. Powder X-ray diffraction measurements were carried out on a Rigaku RU200 diffractometer at 60 kV, 300 mA, and Cu Kα radiation (λ = 1.5406 Å). The gas adsorption properties were studied on an ASAP 2460 surface area analyzer.

Synthesis of $H_3O[In_3(pta)_4(OH)_2]\cdot 10H_2O$ (NXU-1) (CCDC:2101490). A mixture of $In(NO_3)_2\cdot 6H_2O$ (0.25 mmol, 0.0073 g) and H_2pta (0.05 mmol, 0.0122 g) in the mixed H_2O (4mL) and C_2H_5OH (2mL) solvents with pH value adjusted to 8.0 with 60 μL trimethylamine was placed in a Teflon-lined stainless steel vessel (15 mL), heated to 160 °C for 96 h and then cooled to room temperature at a rate of 5 °C h^{-1}. The brown rodlike crystals were obtained and dried in air to give 0.0052 g, yield 62.3% based on In. Anal. Calcd for $C_{52}H_{53}In_3N_4O_{29}$ (1542.46): C, 40.49; H, 3.46; N, 3.63%. Found: C, 40.67; H, 3.55; N, 3.78%. Main IR features (KBr pellet, cm^{-1}): 3399(vs), 3065(s), 1708(vs), 1618(s), 1491(w), 1364(w), 1292(s), 1220(s), 832(m), 750(m), 551(m).

Synthesis of $[In(pta)_2]\cdot C_3H_{10}N$ (NXU-2) (CCDC:2101491). Brown square crystals of **NXU-2** can be obtained following the same synthetic procedure as that for **NXU-1** except that the pH value was adjusted to 5.0 with 30 μL trimethylamine. Anal. Calcd for $C_{29}H_{24}InN_3O_8$ (657.33): C, 52.98; H, 3.68; N, 6.39%. Found: C, 52.19; H, 3.52; N, 6.28%. Main IR features (KBr pellet, cm^{-1}): 3402 (m), 3061 (w), 2924 (m), 1958 (w), 1666 (s), 1583 (s), 1489 (m), 1415 (s), 1351 (s), 1268 (m), 1223 (w), 1095

(w), 863 (w), 769 (m), 582 (w).

Synthesis of $[In(pta)_2]\cdot C_3H_{10}N$ (NXU-3) (CCDC:2101492). The synthetic procedure for **NXU-3** was basically the same as that of **NXU-1** except that the pH of the mixture was measured to 3.0. Anal. Calcd for $C_{29}H_{24}InN_3O_8$ (657.33): C, 52.98%; H, 3.68%; N, 6.39%. Found: C, 52.17%; H, 3.47%; N, 6.22%. Main IR features (KBr pellet, cm^{-1}): 3214(m), 3066(w), 2362(w), 1953(w), 1849(w), 1612(s), 1489(m), 1410(s), 1350(s), 1267(m), 1218(m), 1115(w), 1066(w), 863(m), 769(m), 553(w).

X-ray crystallography

Single-crystal X-ray diffraction data were collected on a Bruker SMART APEX-CCD-based diffractometer using graphite monochromated either Cu (λ = 1.54184 Å) or Ga (λ = 1.34139 Å) radiation. Data processing and absorption corrections were accomplished using SAINT and SADABS.[1] The structures were solved by direct methods and refined against F^2 by fullmatrix least-squares with SHELXTL-2014.[2] All the hydrogen atoms were located at geometrically calculated positions. The diffraction contribution of the highly disordered solvent molecules located in the structure was eliminated by applying the program SQUEEZE implemented in PLATON. The final formula of **NXU-1** - **NXU-3** were ascertained by combining the crystallographic data, elemental microanalyses, and TGA data. The detailed structural refinement results are given in Table S1, and the selected bond lengths and angles are provided in Tables S2-S4.

2. Quantum chemical calculations

For complex **NXU-1**, we have employed the first-principles to perform all density functional theory (DFT) calculations within the generalized gradient approximation (GGA) using the Perdew-Burke-Ernzerhof (PBE) formulation.[3] We have chosen the projected augmented wave (PAW) potentials to describe the ionic cores and take valence electrons into account using a plane wave basis set with a kinetic energy cutoff of 630 eV. Partial occupancies of the Kohn-Sham orbitals were allowed using the Gaussian smearing method and a width of 0.05 eV. The electronic energy was considered self-consistent when the energy change was smaller than 10^{-4} eV. A

geometry optimization was considered convergent when the energy change was smaller than 10^{-6} eV.

Table S1. Selected crystallographic data for complexes **NXU-1**, **NXU-2**, **NXU-3**.

Complex	**NXU-1**	**NXU-2**	**NXU-3**
Empirical formula	$C_{52}H_{30}In_3N_4O_{18}$	$C_{26}H_{14}InN_2O_8$	$C_{26}H_{14}InN_2O_8$
Formula weight	1343.26	643.31	643.30
Temperature	156 K	193 K	193 K
Crystal system	monoclinic	monoclinic	tetragonal
Space group	*P21/n*	*C2/c*	*P42/mbc*
a (Å)	15.2038(2)	26.8733(11)	20.2125(7)
b (Å)	22.6496(3)	20.7854(8)	20.2125(7)
c (Å)	22.0920(3)	22.4567(9)	22.9119(9)
α (°)	90	90	90
β (°)	108.9446(16)	124.201(2)	90
γ (°)	90	90	90
V (Å^3)	7194.95(19)	10374.5(7)	9360.6(7)
Z	4	8	8
D (g/cm^3)	1.240	0.824	0.913
Mu (mm^{-1})	8.109	2.641	2.927
F(0 0 0)	2644.0	2592	2592
Unique reflections	12626	17852	4939
Observed reflections	24333	17852	173822
R_{int}	0.0321	0.0645	0.0664
Final *R* indices	R_1=0.0699	R_1=0.0746	R_1=0.0648
[$I>2\sigma(I)$]	wR_2=0.1928	wR_2=0.2224	wR_2=0.2029
R indices (all data)	R_1=0.0825	R_1=0.1036	R_1=0.0685
	wR_2=0.2051	wR_2=0.2449	wR_2=0.2074
Goodness-of-fit on F^2	1.053	1.075	1.052

Table S2. Selected Bond Lengths (Å) and Bond Angles (°) for **NXU-1**

NXU-1					
In(1)-O(1)	2.107(11)	In(2)-O(9)	2.069(6)	O(1)-In(1)-O(4)#1	173.4(4)
In(1)-O(4)#1	2.172(4)	In(2)-O(3)#4	2.161(5)	O(1)-In(1)-O(5)	89.3(6)
In(1)-O(5)	2.110(3)	In(2)-O(8)#5	2.162(6)	O(5)-In(1)-N(1)#3	90.5(6)
In(1)-O(7)#2	2.185(5)	In(2)-O(9)#6	2.069(6)	O(9)-In(1)-O(1)	89.9(3)
In(1)-O(9)	2.083(5)	O(1)-C(1)	1.154(12)	O(3)#4-In(2)-O(8)#2	91.1(2)
In(1)-N(1)#3	2.232(5)	O(2)-C(1)	1.322(13)	O(9)-In(2)-O(3)#1	92.4(2)

In(2)-O(3)#1	2.161(5)	N(1)-C(10)	1.355(17)	O(9)-In(2)-O(8)#2	90.6(2)
In(2)-O(8)#2	2.162(6)	N(1)-C(11)	1.328(15)	O(9)#6-In(2)-O(8)#5	90.6(2)

#1 -1/2+x,3/2-y,-1/2+z #2 1/2-x,1/2+y,1/2-z #3 1/2-x,3/2-y,1-z #4 1-x,+y,1/2+z #5 +x,1-y,-1/2+z #6 1/2-x,3/2-y,-z

Table S3. Selected Bond Lengths (Å) and Bond Angles (°) for **NXU-2**

NXU-2

In(1)-O(1)	2.121(5)	O(1)-In(1)-O(4)#1	170.8(2)	O(1) -In(1)-O(8)#3	85.41(18)
In(1)-O(4)#1	2.143(5)	O(1)-In(1)-O(6)	104.0(2)	O(6)-In(1)-O(8)#3	141.5(2)
In(1)-O(6)	2.202(5)	O(4)#1-In(1)-O(6)	84.2(2)	N(1)#2-In(1)-O(8)#3	81.09(18)
In(1)-O(7)#3	2.295(5)	O(1)-In(1)-N(1)#2	83.8(2)	N(1)#2-In(1)-O(5)	81.28(18)
In(1)-O(5)	2.336(5)	O(6)-In(1)-N(1)#2	136.38(19)	N(1)#2-In(1)-O(7)#3	136.90(18)
In(1)-N(1)#2	2.2281(6)	O(1)-In(1)-O(5)	83.5(2)	O(5)-In(1)-O(8)#3	160.22(19)
In(2)-O(8)#3	2.348(5)	O(6)-In(1)-O(5)	57.7(2)	O(7)#3-In(1)-O(5)	140.03(19)
O(1)-C(1)	1.272(10)	O(4)#1-In(1)-O(5)	104.67(19)	O(1)-In(1)-O(7)#3	89.3(2)

#1 +x,-1-y,1/2+z #2 1-x,+y,3/2-z #3 1/2-x,1/2+y,3/2-z

Table S4. Selected Bond Lengths (Å) and Bond Angles (°) for **NXU-3**

NXU-3

In(1)-O(1)#3	2.197(5)	O(1)#3-In(1)-O(4)		O(1)#2-In(1)-O(5)	
In(1)-O(4)	2.246(6)	O(5)-In(1)-O(4)		O(1)#2-In(1)-O(2)#3	
In(1)-O(5)	2.241(6)	O(5)-In(1)-N(1)#4		C(11)-N(1)-C12	118.5(7)
In(1)-N(1)#4	2.256(6)	O(4)-In(1)-N(1)#4		C(11)-N(1)-In(1)#4	122.0(5)
In(1)-O(2)#3	2.419(5)	O(5)-In(1)-O(2)#3		C(12)-N(1)-In(1)#4	119.5(5)
In(1)-O(1)#2	2.130(5)	O(1)#3-In(1)-O(2)#3		C(1)-O(1)-In(1)#1	95.9(4)
O(1)-C(1)	1.265(8)	O(4)-In(1)-O(2)#3		C(8)-O(4)-In(1)	95.0(5)
O(2)-C(1)	1.236(8)	C(8)-O(5)-In(1)		N(1)#4-In(1)-O(2)#3	

#1 1/2-x,-1/2+y,1-z #2 +x,+y,1-z #3 1/2-x,1/2+y,1-z #4 -x,1-y,1-z

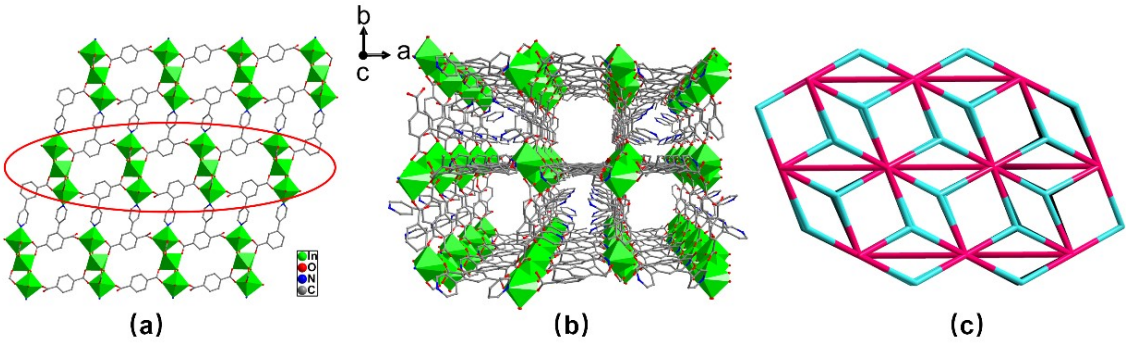

Figure S1. (a) 2D view of a structural fragment of **NXU-1**; (b) 3D structure of **NXU-**

1 along the c axis; (c) View of the (3,10)-connected topological network for **NXU-1**.

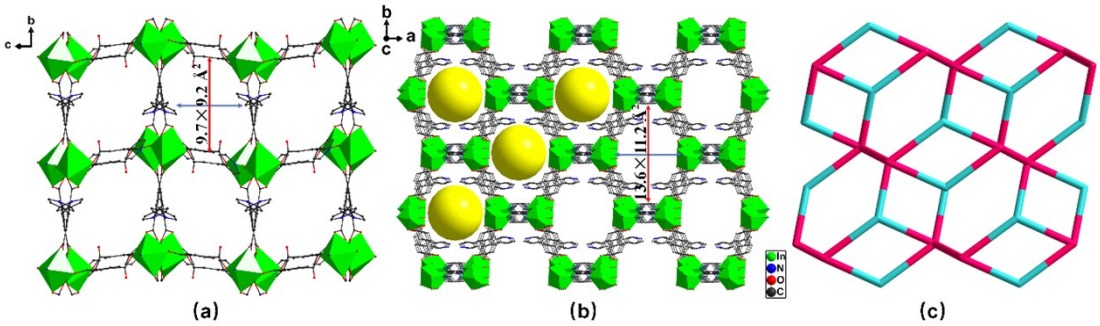

Figure S2. (a) 3D structure of **NXU-2** viewed along the a axis; (b) 3D structure of **NXU-2** with 1D channels along the c axis; (c) View of the (3,5)-connected topological network for **NXU-2**.

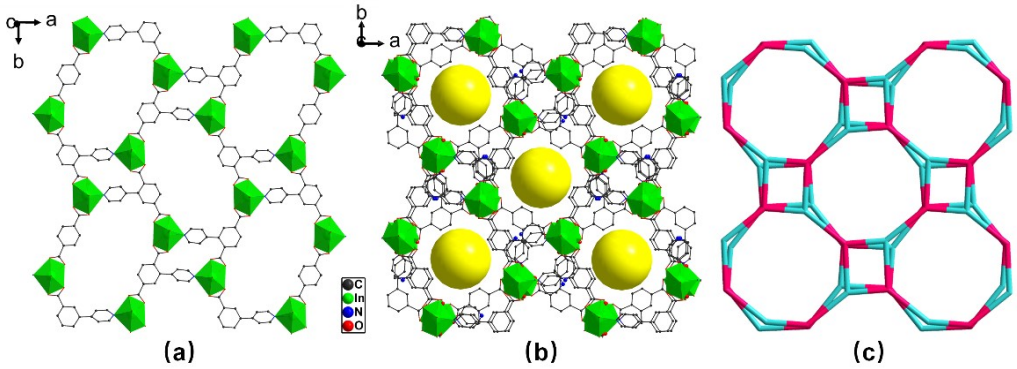

Figure S3. (a) 2D view of a structural fragment of **NXU-3** along the c-axis; (b) 3D structure of **NXU-3** with 1D channels along the c-axis; (c) View of the (3,5)-connected topological network for **NXU-3**.

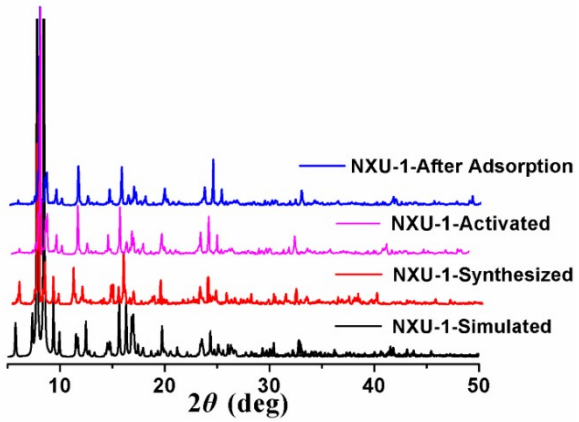

Figure S4. PXRD pattern of **NXU-1** simulated from the X-ray single-crystal structure, as-synthesized, activated and after adsorption sample.

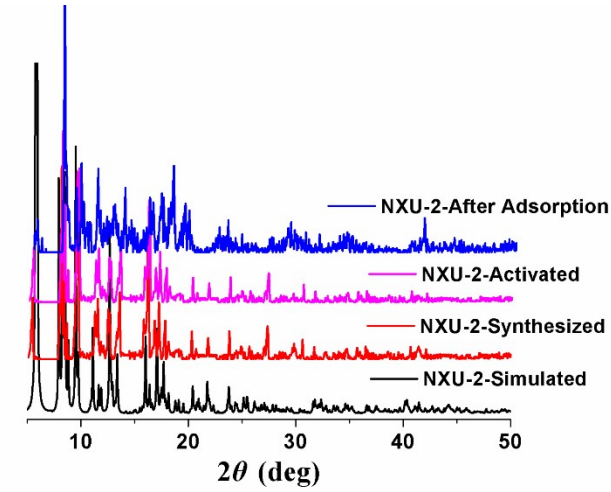

Figure S5. PXRD pattern of **NXU-2** simulated from the X-ray single-crystal structure, as-synthesized, activated and after adsorption sample.

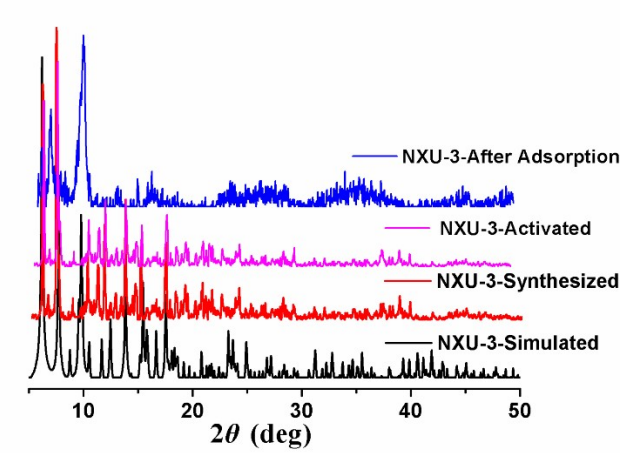

Figure S6. PXRD pattern of **NXU-3** simulated from the X-ray single-crystal structure, as-synthesized, activated and after adsorption sample.

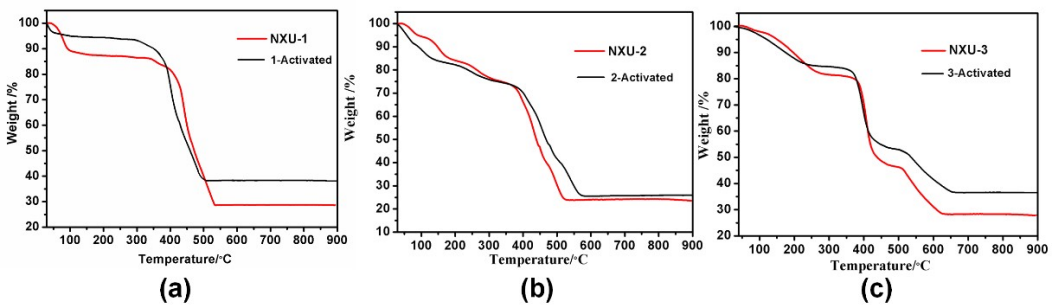

Figure S7. TGA plots of **NXU-1** (a), **NXU-2** (b) and **NXU-3** (c) under a N_2 environment.

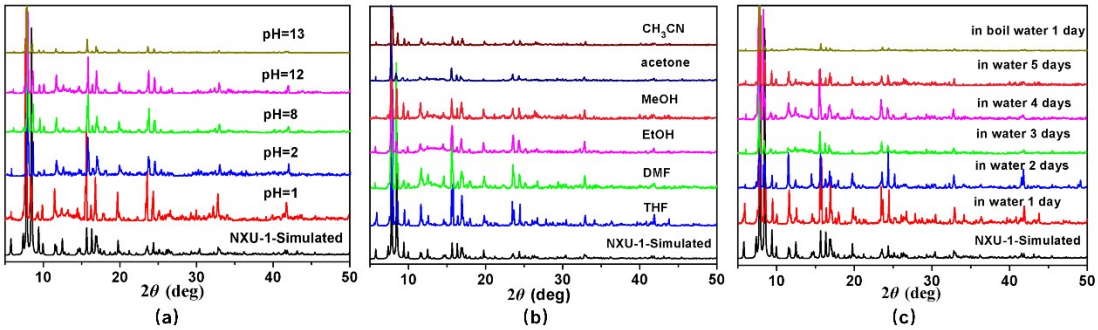

Figure S8. PXRD profiles of **NXU-1** after being soaked in acidic and basic solutions (a), different solvents (b) and water (c).

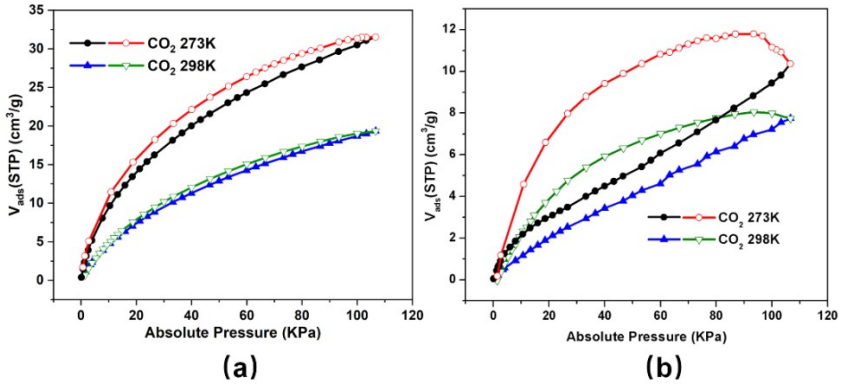

Figure S9. CO_2 sorption isotherms of **NXU-2** (a) and **NXU-3** (b) at 273 and 298 K.

IAST adsorption selectivity calculation:

The experimental isotherm data for pure CO_2 and CH_4 (measured at 298) were fitted using a dual Langmuir-Freundlich (L-F) model:

$$q = \frac{a_1 * b_1 * p^{1/c1}}{1 + b_1 * p^{1/c1}} + \frac{a_2 * b_2 * p^{1/c2}}{1 + b_1 * p^{1/c1}}$$

Where q and p are adsorbed amounts and pressures of component i, respectively.

The adsorption selectivity for binary mixtures of CO_2/CH_4, defined by

$$S_{i/j} = \frac{x_i * y_j}{x_j * y_i}$$

were calculated using the Ideal Adsorption Solution Theory (IAST) of Myers and Prausnitz.

Where x_i is the mole fraction of component i in the adsorbed phase and y_i is the mole fraction of component i in the bulk.

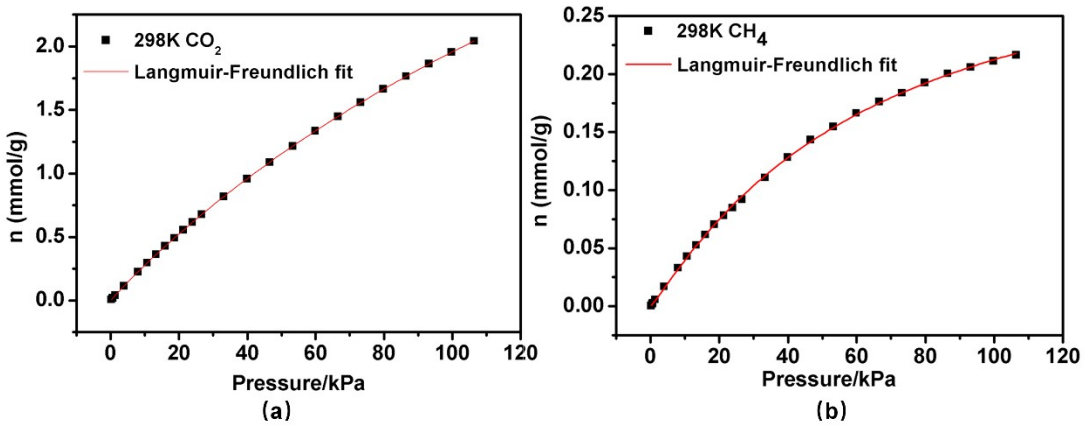

Figure S10. CO_2 adsorption isotherms of **NXU-1** with fitting by L-F model: a_1 = 7.0273, b_1 = 0.0043, c_1 = 0.9737, R^2 = 1; CH_4 adsorption isotherms of **NXU-1** with fitting by L-F model: a_1= 0.343, b_1 = 0.010, c_1 = 1.093, R^2 = 0.99974.

Calculation of sorption heat for CO_2 and CH_4 uptakes using Virial 2 model

$$\ln p = \ln N + 1/T \sum_{i=0}^{m} aiN^i + \sum_{i=0}^{n} biN^i \qquad Q_{st} = -R \sum_{i=0}^{m} aiN^i$$

The above equation was applied to fit the combined CO_2 and CH_4 isotherm data for **NXU-1** at 273 and 298 K, where *P* is the pressure, *N* is the adsorbed amount, *T* is the temperature, *ai* and *bi* are virial coefficients, and *m* and *n* are the number of coefficients used to describe the isotherms. Q_{st} is the coverage-dependent enthalpy of

adsorption and *R* is the universal gas constant.

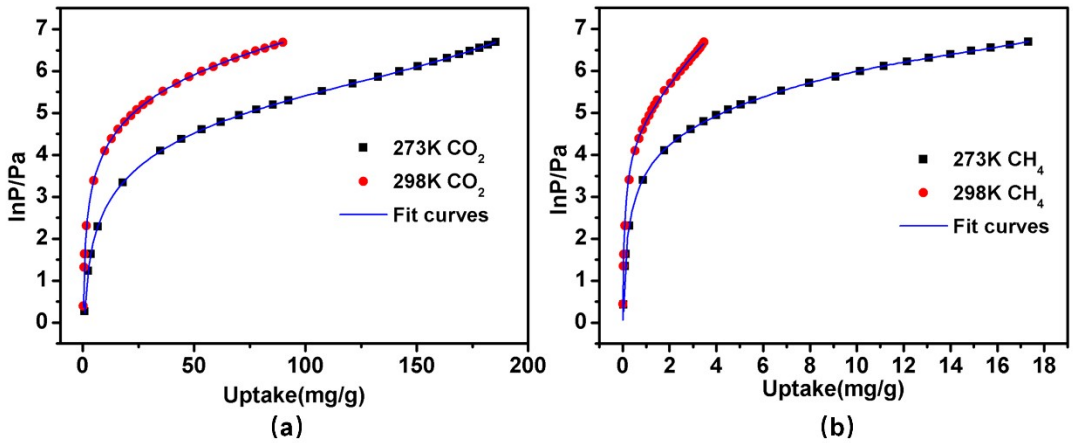

Figure S11. CO_2 adsorption isotherms for **NXU-1** with fitting by Virial 2 model. Fitting results: a_0 = -4620.16743, a_1 = 4.03007, a_2 = -0.04718, a_3 = 6.56431 × 10^{-6}, a_4 = -1.17051 × 10^{-7}, b_0 = 17.25724, b_1 = -0.00788, b_2 = 1.38908 × 10^{-4}, b_3 = 5.61989 × 10^{-8}, R^2 = 0.99997; CH_4 adsorption isotherms for **NXU-1** with fitting by Virial 2 model. Fitting results: a_0 = -4051.51954, a_1 = 560.9957, a_2 = -561.78977, a_3 = 66.67458, a_4 = 0.00838, b_0 = 16.46272, b_1 =-2.12285, b_2 = 2.07434, b_3 = -0.24544, R^2 = 0.998.

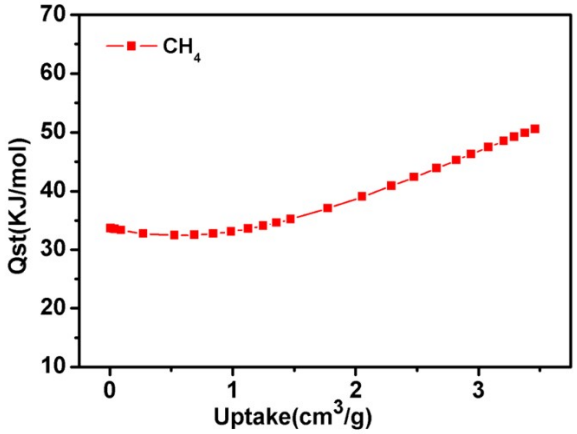

Figure S12. Adsorption enthalpies of CH_4 for **NXU-1**.

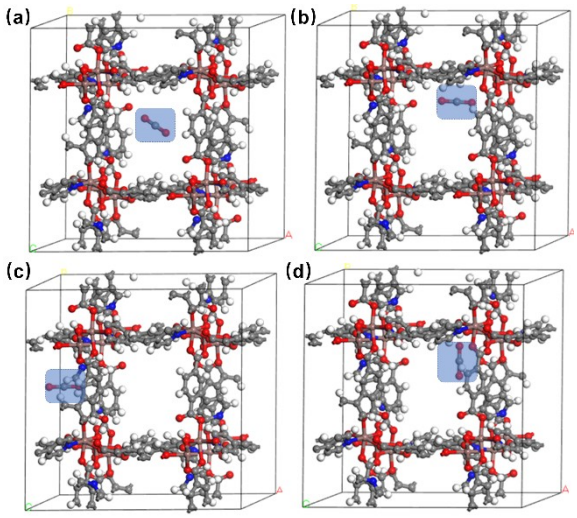

Figure S13. Optimized binding sites for CO_2 in **NXU-1**., C, gray; In, brown; O, red; N, blue.

3. References

1. Sheldrick, G. M. *SADABS: Program for Empirical Absorption Correction;* University of G**ö**ttingen: G**ö**ttingen, Germany, 1996.
2. Sheldrick, G. M. *SHELXS-2014 and SHELXL-2014: Program for Crystal Structure Determination*; University of G**ö**ttingen: G**ö**ttingen, Germany, 2014.
3. S. Xiang, H. Huang, and L. M. Hsiung. *Journal of nuclear materials*, 2008, **375**, 113-119.